ORGANOMETALLICS

Article

The Linear Tetraphos Ligand prP (1,1,4,8,11,11-Hexaphenyl-1,4,8,11-tetraphosphaundecane, PhPCHCHP(Ph)CHCHCHP(Ph)CHCHPPh): Synthesis and Characterization of *cis*- and *trans*-[Fe(NCS)(prP)]

Carsten M. Habeck, Christian Hoberg, Gerhard Peters, Christian Nther, and Felix Tuczek

Organometallics, **2004**, 23 (13), 3252-3258 • DOI: 10.1021/om030579k

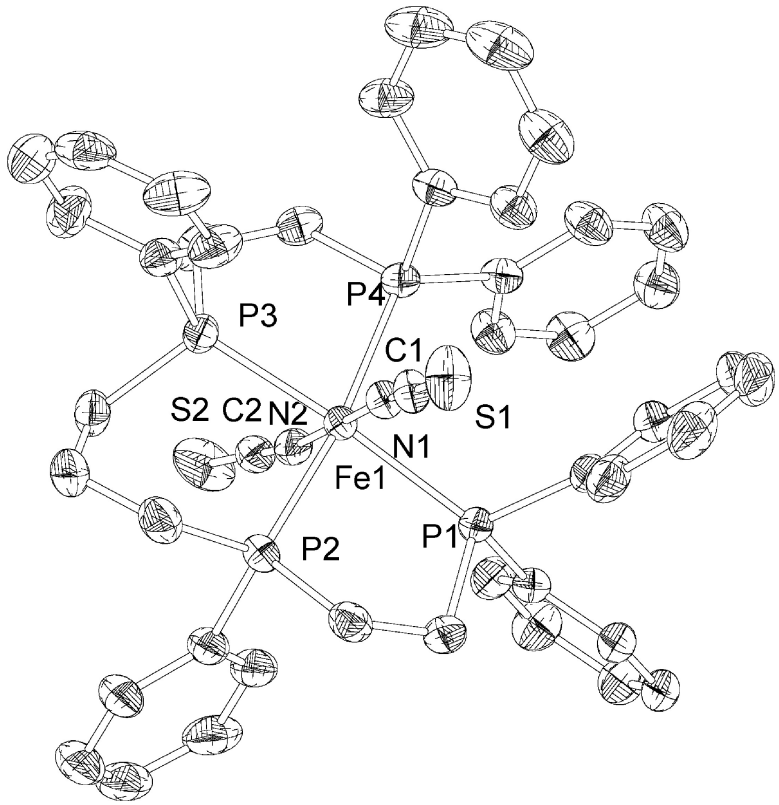

More About This Article

Additional resources and features associated with this article are available within the HTML version:

- Supporting Information
- Access to high resolution figures
- Links to articles and content related to this article

The Linear Tetraphos Ligand prP_4 (1,1,4,8,11,11-Hexaphenyl-1,4,8,11-tetraphosphaundecane, $Ph_2PCH_2CH_2P(Ph)CH_2CH_2CH_2P(Ph)CH_2CH_2PPh_2$): Synthesis and Characterization of *cis*- and *trans*-$[Fe(NCS)_2(prP_4)]$†

Carsten M. Habeck, Christian Hoberg, Gerhard Peters, Christian Näther, and Felix Tuczek*

Institut für Anorganische Chemie, Christian-Albrechts-Universität Kiel, D-24098 Kiel, Germany

Received August 13, 2003

The stereochemistry of prP_4 (1,1,4,8,11,11-hexaphenyl-1,4,8,11-tetraphosphaundecane) and its coordination properties in mononuclear complexes are explored. The free ligand is obtained as a mixture of *meso* and *rac* diastereomers from the reaction of dilithium 1,3-bis(phenylphosphido)propane−tetrakis(tetrahydrofuran) ("Lippp") with 2 equiv of 1-chloro-2-(diphenylphosphino)ethane. Reaction of prP_4 with $FeCl_2$ and KSCN leads to *cis*- and *trans*-$[Fe(NCS)_2(prP_4)]$ complexes of the *meso* and the *rac* ligands; the composition of this mixture has been fully analyzed. The iron isothiocyanato complexes *cis*-α- and *trans*-$[Fe(NCS)_2(rac\text{-}prP_4)]$ have been characterized by X-ray structure determinations. The ^{31}P NMR spectrum of the free tetraphos ligand shows an AA′XX′ coupling scheme with three groups of signals centered at −20.6 and −20.7 ppm and at −12.4 ppm, which belong to the *rac* and *meso* isomers, respectively. ^{31}P NMR spectra of the *cis* and *trans* iron isothiocyanato complexes of *rac*-prP_4 exhibit AA′XX′ patterns as well, which can be reproduced by simulation. *trans*-$[Fe(NCS)_2(meso\text{-}prP_4)]$ is identified by its ^{31}P NMR spectrum, which is similar to that of its *rac* counterpart. On the basis of NMR spectroscopy it is found that the *cis*-α complex of the *rac* ligand converts into the *trans-rac* complex with a half-life of approximately 2 days. Infrared and Raman spectra of the *cis*-α and *trans* isomers of $[Fe(NCS)_2(rac\text{-}prP_4)]$ reveal characteristic differences in the region of the C−N stretching vibrations.

Introduction

Since King and Kapoor's pioneering study on the synthesis and ligation properties of the tetradentate ligand tetraphos-I (1,1,4,7,10,10-hexaphenyl-1,4,7,10-tetraphosphadecane), many investigations of this ligand and its transition-metal complexes have been performed.[1] In contrast, only a handful of studies on the analogous tetradentate phosphine ligand 1,1,4,8,11,11-hexaphenyl-1,4,8,11-tetraphosphaundecane ("prP_4"), possessing a central C_3 group, have appeared.[2] We are interested in this ligand as a potential alternative to the bidentate ligands dppe (bis(diphenylphosphino)-ethane) and depe (bis(diethylphosphino)ethane), which have been employed in the field of synthetic nitrogen fixation as coligands of molybdenum and tungsten dinitrogen complexes.[3] A problem with these systems and their counterparts possessing monodentate phosphine ligands is the breaking of phosphine−metal bonds at the NNH_2 and NNH_3 stages of the conversion of coordinated N_2 to NH_3.[3a,d] With respect to the construction of a catalytic cycle based upon the "P_4 platform",[4] however, maximum stability of the equatorial phosphine ligation is desirable. Employing a tetradentate ligand such as prP_4 in Mo/W dinitrogen systems might be a promising strategy toward this goal. So far, however, only binuclear complexes of prP_4 have been prepared.[2a]

In the present paper, the stereochemistry of prP_4 and its coordination properties in mononuclear complexes are explored. To this end, iron thiocyanato complexes of prP_4 have been synthesized and characterized both structurally and spectroscopically. Iron complexes of tetraphos-I have been investigated intensively.[1a,c,e] In analogy to this ligand, prP_4 is expected to have three

† Dedicated to Prof. Dr. G.-V. Röschenthaler on the occasion of his 60th anniversary.

* To whom correspondence should be addressed. E-mail: ftuczek@ac.uni-kiel.de. Fax: +49 431 880 1520.

(1) (a) King, R. B.; Kapoor, R. N.; Saran, M. S.; Kapoor, P. N. *Inorg. Chem.* **1971**, *10*(9), 1851. (b) Bautista, M. T.; Earl, K. A.; Maltby, P. A.; Morris, R. H. *Can. J. Chem.* **1994**, *72*, 547. (c) Ghilardi, C. A.; Midollini, S.; Sacconi, L.; Stoppioni, P. *J. Organomet. Chem.* **1981**, *205*, 193. (d) Goller, H.; Brüggeller, P. *Inorg. Chim. Acta* **1992**, *197*, 75. (e) Bacci, M.; Midollini, S.; Stoppioni, P.; Sacconi, L. *Inorg. Chem.* **1973**, *12*(8), 1801. (f) Oberhauser, W.; Bachmann, C.; Brüggeller, P. *Polyhedron* **1995**, *14*(6), 787. (g) Brüggeller, P. *Inorg. Chim. Acta* **1989**, *155*, 45. (h) Chen, J−D.; Cotton, F. A.; Hong, B. *Inorg. Chem.* **1993**, *32*, 2343. (i) King, R. B.; Kapoor, P. N. *J. Am. Chem. Soc.* **1971**, *93*(17), 4158.

(2) (a) Brown, J. M.; Canning, L. R. *J. Organomet. Chem.* **1984**, *267*, 179. (b) DuBois, D. L.; Myers, W. H.; Meek, D. W. *J. Chem. Soc., Dalton Trans.* **1975**, 1011.

(3) (a) Henderson, R. A.; Leigh, G. J.; Pickett, C. J. *Adv. Inorg. Radiochem.* **1983**, *27*, 197. (b) Fryzuk, M.; Johnson, S. A. *Coord. Chem. Rev.* **2000**, *200*, 379. (c) Hidai, M.; Mizobe, Y. *Chem. Rev.* **1995**, *95*, 1115. (d) Horn, K. H.; Lehnert, N.; Tuczek, F. *Inorg. Chem.* **2003**, *42*, 1076.

(4) Alias, Y.; Ibrahim, S. K.; Queiros, M. A.; Fonseca, A.; Talarmin, J.; Volant, F.; Pickett, C. J. *J. Chem. Soc., Dalton Trans.* **1997**, 4807.

10.1021/om030579k CCC: $27.50
Publication on Web 05/27/2004

Chart 1. *meso* and *rac* Isomers of the prP_4 Ligand

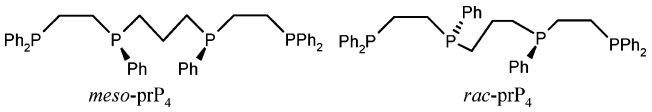

Chart 2. Possible Isomers for Octahedral prP_4 Complexes

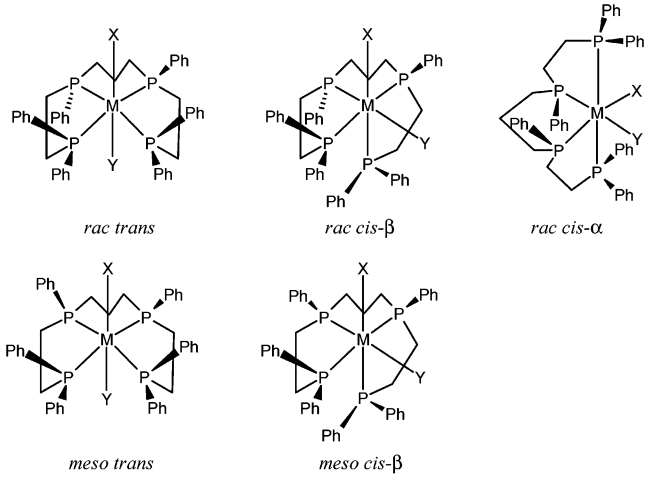

isomers, one *meso* and one *rac* diastereomer, the latter existing as a racemic mixture of two enantiomers (Chart 1). The two asymmetric phosphorus atoms in the the *meso* compound exhibit *R,S* and *S,R* configurations, respectively, whereas the stereoisomers of the *rac* compound have *R,R* and *S,S* configurations at the asymmetric P atoms, respectively. In further analogy to tetraphos-I, the *rac* isomer of the ligand can form octahedral complexes in three different ways: *cis*-α, *cis*-*β*, and *trans* (Chart 2).[5] Owing to steric reasons, the *meso* ligand has only two possibilities to form octahedral complexes: *trans*- and *cis*-*β*. Reacting prP_4 with $FeCl_2$ and 2 equiv of KSCN afforded the complexes *trans*-[Fe(NCS)$_2$(*rac*-prP_4)] (**1**), *trans*-[Fe(NCS)$_2$(*rac*-prP_4)]·CH_2Cl_2 (**2**), and *cis*-α-[Fe(NCS)$_2$(*rac*-*prP*$_4$)]·CH_2Cl_2 (**3**), as well as *trans*-[Fe(NCS)$_2$(*meso*-prP_4)] (**4**). **1**−**3** were characterized by single-crystal X-ray structure analyses and by ^{31}P NMR as well as optical and vibrational spectroscopy. Evidence for the formation of complex **4** was obtained by ^{31}P NMR. Here the structural and spectroscopic properties of **1**−**4** are presented and the consequences with respect to the coordination properties of prP_4 are discussed.

Results and Discussion

Synthesis and Spectroscopic Properties of prP_4. The prP_4 ligand was prepared in analogy to a published synthesis of tetraphos-I (Scheme 1).[1b] Like this ligand, prP_4 exists in two isomeric forms, *meso* and *rac* (vide supra). In analogy to the synthesis of tetraphos-I giving 70% *meso* and 30% *rac*, the preparation of prP_4 leads to a mixture of both isomers, however, with varying proportions. This result is in contrast to previous reports on the synthesis of prP_4 (however, by different routes), where formation of only one isomer was claimed. The identity of this isomer, however, was not specified.[2] To conserve the original isomeric composition of the prP_4 ligand, we refrained from subsequent pyrolysis of the reaction product as performed by various authors.[1d,f,2a] Spectroscopic and structural characterization of the free ligand and its iron thiocyanato complexes are presented in the following sections.

Scheme 1. Synthetic Route for the prP_4 Ligand

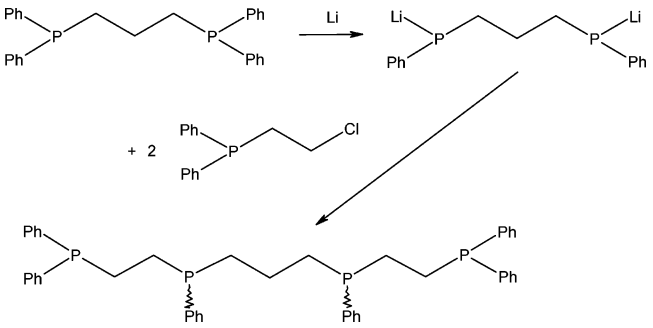

NMR Spectroscopy and Spectral Simulation of Free prP_4. The ^{31}P NMR spectrum of the free prP_4 ligand shows three groups of signals corresponding to two isomers (Figure 1). Each isomer gives a four-line spectrum consisting of two doublets. Because of the higher shielding of the alkyl as compared to the phenyl groups, the signals at ~ -20 ppm are assigned to the spins of the asymmetric phosphorus atoms and the signals at −12.4 ppm to the terminal ones. This assignment is supported by the fact that the signals of the latter atoms have identical shifts in both isomers and therefore are superposed, whereas the doublets of the asymmetric P atoms exhibit slightly different chemical shifts (−20.6 and −20.7 ppm), resulting in a four-line group. On the basis of the relative NMR intensities of the various [Fe(NCS)$_2$(prP_4)] complexes prepared from the diastereomeric ligand mixture of Figure 1 (see below), the pair of signals at lower field (high intensity) is assigned to the *meso* isomer of prP_4. As shown in Figure 1, the spectrum of each isomer can be simulated on the basis of an AA′XX′ system with the coupling constants for the AX and A′X′ interactions being 29 Hz, respectively, and all other constants being 0.[2b]

Primary Reaction Product with [Fe(NCS)$_2$]. To further characterize the prP_4 ligand and define its stereochemistry, complexes with iron(II) and thiocyanate were prepared. The ^{31}P NMR spectrum of the primary reaction product of $FeCl_2$, KSCN, and prP_4 indicates the presence of three species, each of which gives rise to two multiplets (Figure 2). The various subspectra could be assigned to specific isomers of [Fe(NCS)$_2$(prP_4)] on the basis of fractional crystallization of the three *trans* and *cis* bis(isothiocyanato)iron complexes *trans*-[Fe(NCS)$_2$(*rac*-prP_4)] (**1**), *trans*-[Fe(NCS)$_2$(*rac*-prP_4)]·CH_2Cl_2 (**2**), and *cis*-α-[Fe(NCS)$_2$(*rac*-prP_4)]·CH_2Cl_2 (**3**) and measurement of their individual NMR spectra. Here the crystal structures of **1**−**3** are reported and their ^{31}P NMR spectra are discussed.

Structures of *trans*-[Fe(NCS)$_2$(*rac*-prP_4)] (1) and *trans*-[Fe(NCS)$_2$(*rac*-prP_4)]·CH_2Cl_2 (2). The first species could be identified as the *trans*-*rac* isomer found in the two pseudopolymorphic forms **1** and **2** which cocrystallize from concentrated solutions of the primary reaction product. Complex **1** has the rhombohedral

(5) (a) Bosnich, B.; Jackson, W. G.; Wild, S. B. *J. Am. Chem. Soc.* **1973**, *95*, 8269. (b) Gavrilova, A. L.; Bosnich, B. *Chem. Rev.* **2004**, *104*, 349.

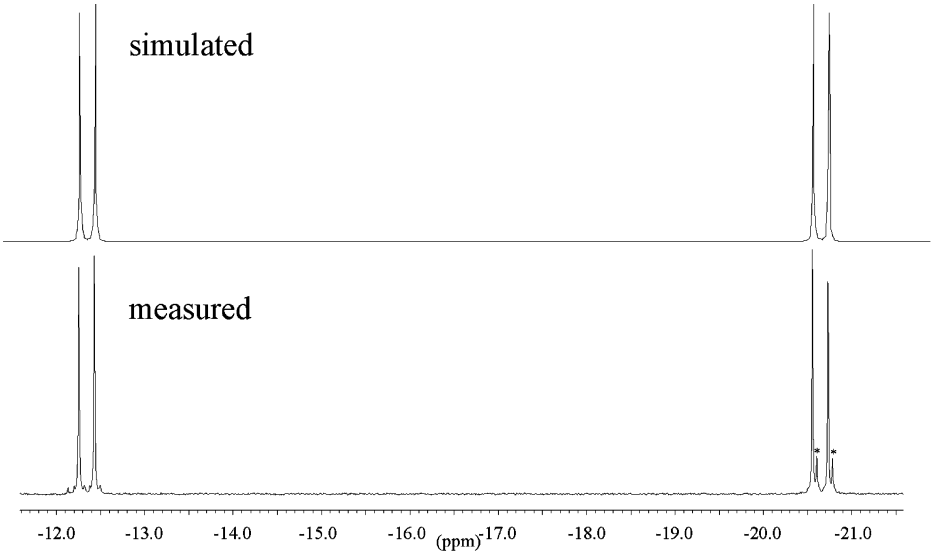

Figure 1. Experimental (bottom) and simulated (top) ^{31}P NMR spectra of prP_4 (asterisks mark the signals of the *rac* isomer).

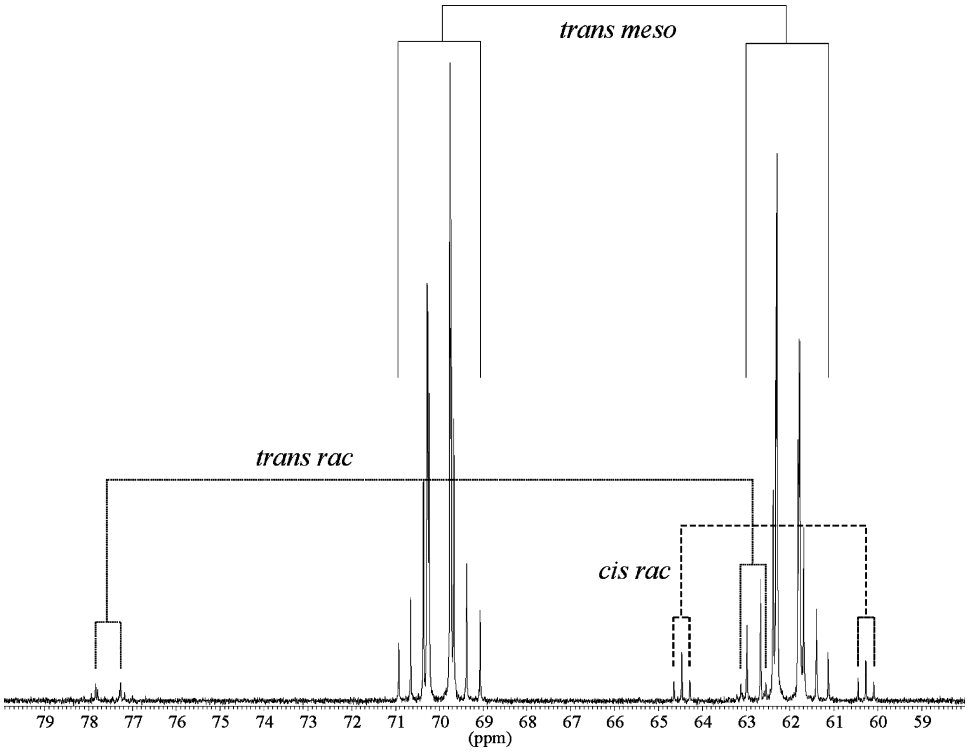

Figure 2. ^{31}P NMR spectra of the primary reaction product of $FeCl_2$ with prP_4 and 2 equiv of KSCN, containing three different isomers.

space group $R\bar{3}$, whereas crystals of **2** have the monoclinic space group $P2_1/c$ (Table 1). In both complexes the thiocyanate ligands are bound through the nitrogen atoms (Figure 3). Important bond lengths and angles for all complexes are collected in Table 2. The average Fe−N bond lengths are ∼1.93 Å in both complexes, and the P−Fe bond lengths are between 2.238(1) and 2.310(1) Å. The N−Fe−N angle is 178.56(6)° for **1** and 174.58(6)° for **2**. The two thiocyanate groups are almost linear; i.e., the S−C−N angles are 179.0° for **1** and 178.4(2)° for **2**. The N−C bonds have an average length of about 1.16 Å, and the C−S bond lengths are ∼1.63 Å. Fe−N−C angles have values of 176.0(2) and 171.9(2)° for **1** and 175.5(2) and 167.4(2)° for **2**.

NMR Spectra and Spectral Simulation of *trans*-[Fe(NCS)$_2$(prP$_4$)]. The spectrum of the pure complex *trans*-[Fe(NCS)$_2$(*rac*-prP$_4$)] is shown in Figure 4. As in case of the ^{31}P NMR spectrum of free prP_4, the spectrum can be interpreted on the basis of an AA′XX′ coupling scheme. There are two groups of signals, both multiplets, centered at 77.5 and 62.6 ppm. The peaks at 62.6 ppm are caused by the spins of the asymmetric (inner) phosphorus atoms, whereas the multiplet at 77.5 ppm is derived from the terminal P atoms. Simulation with the coupling constants given in Table 3 shows very good agreement with the measured spectrum (Figure 4). The *cis* coupling constant between the A and X spins has a value of −26 Hz. With 112 Hz (A/X′ and A′/X) the

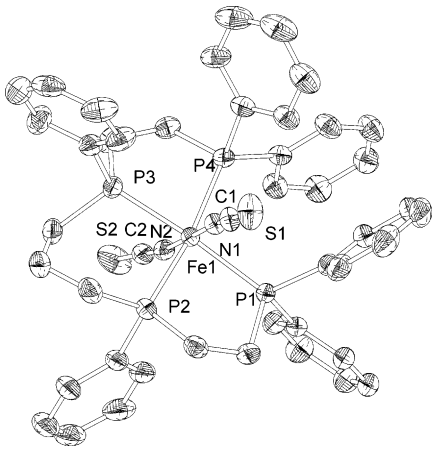

Figure 3. Single-crystal structure of *trans*-[Fe(NCS)$_2$(*rac*-prP$_4$)] (**1**) with the labeling scheme.

Table 1. Crystallographic Data for *trans*-[Fe(NCS)$_2$(*rac*-prP$_4$)] (1), *trans*-[Fe(NCS)$_2$(*rac*-prP$_4$)]·CH$_2$Cl$_2$ (2), and *cis*-α-[Fe(NCS)$_2$(*rac*-prP$_4$)]·CH$_2$Cl$_2$ (3)

	1	2	3
chem formula	$C_{45}H_{44}N_2FeS_2$	$C_{46}H_{46}N_2FeS_2Cl_2$	$C_{46}H_{46}N_2FeS_2Cl_2$
mol wt	856.67	941.6	941.6
cryst color	red	red	red
cryst syst	rhombohedral	monoclinic	triclinic
space group	$R\bar{3}$	$P2_1/c$	$P\bar{1}$
a/Å	21.107(1)	13.360(1)	9.4592(8)
b/Å	21.107(1)	17.393(1)	13.488(1)
c/Å	49.945(3)	20.196(2)	18.659(2)
α/deg	90	90	102.40(1)
β/deg	90	108.46(1)	99.726(1)
γ/deg	120	90	105.89(1)
V/Å^3	19 271(2)	4451.5(6)	2169.6(2)
Z	18	4	2
D_{calcd}/g cm^{-3}	1.329	1.405	1.441
2θ range/deg	3−52	3−56	3−56
μ/mm^{-1}	0.63	0.73	0.75
T/K	150	150	150
no. of measd rflns	47 627	41 427	21 170
R_{int}	0.0312	0.0370	0.0273
no. of indep rflns	9253	10 645	10 252
no. of rflns with $F_o > 4\sigma(F_o)$	8058	9061	8220
no. of params	488	533	519
R1 ($F_o > 4\sigma(F_o)$)	0.0369	0.0346	0.0329
wR2 (all data)	0.1023	0.0934	0.0864
GOF	1.040	1.0136	1.014
resid electron dens/e/Å^3	0.42/−0.36	1.21/−1.12	0.36/−0.84

constant for the *trans* coupling is greater than for the *cis* coupling, and the remaining *cis* couplings between the X/X′ and A/A′ atoms correspond to ±32 and ±62 Hz, respectively.

Structure of *cis*-α-[Fe(NCS)$_2$(*rac*-prP$_4$)] (3). The *cis* complex **3** crystallizes in the triclinic space group $P\bar{1}$ with two formula units in the unit cell (Table 2). Fe−P bond lengths in this complex are comparable to those in the two *trans*-pseudopolymorphs **1** and **2** (Table 2). The Fe−N bond lengths of 1.964(2) and 1.973(2) Å in **3** are somewhat longer than the corresponding bonds in the *trans* complexes **1** and **2**. The two C−N bond lengths are 1.167(2) Å, and the C−S bond lengths are 1.634(2) and 1.641(2) Å, respectively. The angle between the two *cis*-coordinated nitrogen atoms of 88.99(6)° deviates only slightly from 90° (Figure 5). The angles between the *trans* standing atoms N2 and P3 and between N1 and P2 are 168.83(5) and 174.36(4)°, respectively.

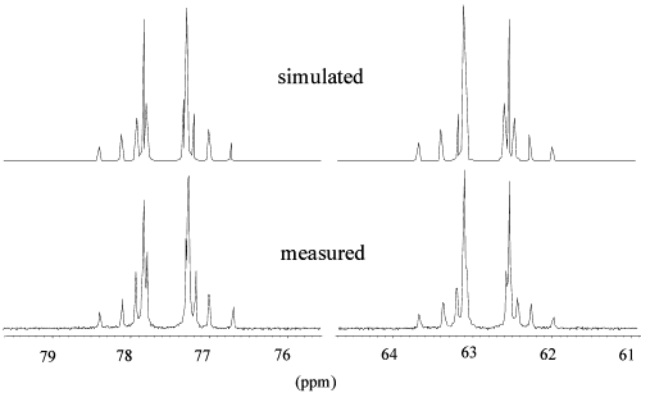

Figure 4. Experimental (bottom) and simulated (top) ^{31}P NMR spectra of *trans*-[Fe(NCS)$_2$(*rac*-prP$_4$)] (**1**).

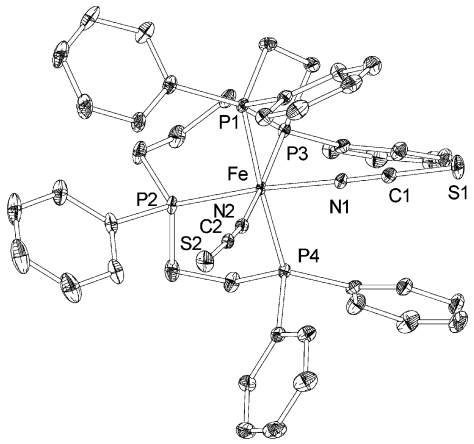

Figure 5. Single-crystal structure of *cis*-α-[Fe(NCS)$_2$(*rac*-prP$_4$)] (**3**) with the labeling scheme.

Table 2. Selected Bond Lengths (Å) and Angles (deg) for *trans*-[Fe(NCS)$_2$(*rac*-prP$_4$)] (1), *trans*-[Fe(NCS)$_2$(*rac*-prP$_4$)]·CH$_2$Cl$_2$ (2), and *cis*-α-[Fe(NCS)$_2$(*rac*-prP$_4$)]·CH$_2$Cl$_2$ (3)

	1	2		3
Fe−N1	1.932(2)	1.933(2)	Fe−N1	1.973(2)
Fe−N2	1.933(2)	1.935(2)	Fe−N2	1.964(2)
S1−C1	1.629(2)	1.629(2)	S1−C1	1.641(2)
S2−C2	1.634(2)	1.636(2)	S2−C2	1.634(2)
C−N1	1.164(2)	1.166(2)	C−N1	1.167(2)
C−N2	1.167(2)	1.169(2)	C−N2	1.167(2)
Fe−P1	2.300(1)	2.302(1)	Fe−P1	2.288(1)
Fe−P2	2.238(1)	2.243(1)	Fe−P2	2.248(6)
Fe−P3	2.261(1)	2.249(1)	Fe−P3	2.238(5)
Fe−P4	2.265(1)	2.310(1)	Fe−P4	2.300(1)
N1−Fe−N2	178.56(6)	174.58(6)	N1−Fe−N2	88.99(6)
Fe−N1−C1	176.0(2)	167.4(2)	Fe−N1−C	176.5(2)
Fe−N2−C2	171.9(2)	175.5(2)	Fe−N2−C	170.9(2)
P1−Fe−P3	174.22(2)	172.37(2)	N1−Fe−P2	174.36(5)
P2−Fe−P4	172.04(2)	174.07(2)	N2−Fe−P3	168.83(5)
N2−Fe−P3	83.44(4)	84.45(4)	P1−Fe− P4	176.34(2)

Table 3. Coupling Constants for ^{31}P Spectra of *trans*-[Fe(NCS)$_2$(*rac*-prP$_4$)]

coupling constant	value (Hz)
$J_{AX} = J_{A'X'}$	−26
$J_{AX'} = J_{A'X}$	112
$J_{XX'}$	±62
$J_{AA'}$	±32

NMR Spectra and Spectral Simulation of *cis*-α-[Fe(NCS)$_2$(*rac*-prP$_4$)] (3). The second species in the

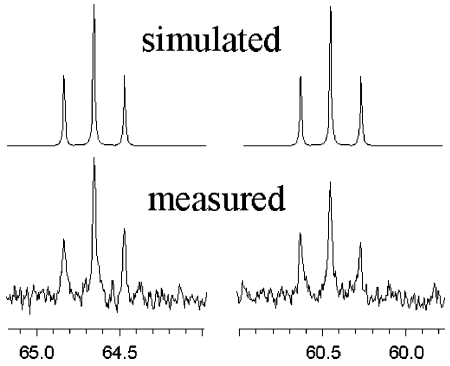

Figure 6. Simulated (top) and experimental (bottom) ^{31}P NMR spectra of *cis*-α-[Fe(NCS)$_2$(*rac*-prP$_4$)] (**3**).

^{31}P NMR spectrum of the primary reaction product has been identified by comparison with the spectrum of pure *cis*-α-[Fe(NCS)$_2$(*rac*-prP$_4$)]. Time-dependent ^{31}P NMR spectroscopy of the pure *cis*-α compound indicates that the *cis* compound slowly (with a half-life of 2 days) converts to the corresponding *trans* complex in solution (see Figure S1 in the Supporting Information), demonstrating that the *trans* geometry of **1** and **2** is slightly favored over the *cis*-α geometry found in **3**. This result is in qualitative agreement with DFT calculations on *trans*- and *cis*-[Fe(NCS)$_2$(H$_2$P(CH$_2$)$_2$P(CH$_2$)$_3$P(CH$_2$)$_2$-PH$_2$)] being models for **1**/**2** and **3**, respectively. These calculations indicate that the *trans* complex is by 5.5 kcal/mol lower in energy than the *cis* complex (see the Supporting Information).

As is evident from Figure 6, the ^{31}P NMR spectrum of *cis*-α-[Fe(NCS)$_2$(*rac*-prP$_4$)] exhibits two signals of triplet appearance located at 60.0 and 64.4 ppm, respectively. In analogy to the ^{31}P spectrum of, for example, *cis*-[Rh(H)$_2$(*rac*-tetraphos-I)]$^+$,[2a] this spectral pattern can be simulated on the basis of an AA′XX′ scheme with one *cis* P−P coupling constant for AX, A′X′, AX′, and A′X (29 Hz; Figure 6).

NMR Spectra and Spectral Simulation of *trans*-[Fe(NCS)$_2$(*meso*-prP$_4$)] (4). The third species in the primary reaction product exhibits a spectral pattern similar to that of the *trans*-*rac* compound: however, with different chemical shifts (center shifts 70 and 62 ppm vs 62.8 and 77.5 ppm in *trans*-*rac*; Figure 7). This spectrum, which corresponds to the major species in Figure 1, is therefore assigned to the *trans*-*meso* isomer **4**. As recrystallization of the primary reaction product primarily gives the *trans*-*rac* compounds **1** and **2** (vide supra), the solubility of the *trans*-*meso* isomer must be higher than that of its *trans*-*rac* counterpart. Notably, there is no indication in the primary reaction product for the presence of the *cis*-*β* isomers, which in principle could be formed by both *meso*- and *rac*-prP$_4$. The ^{31}P NMR spectra of these isomers of [Fe(NCS)$_2$(prP$_4$)] should be qualitatively different from either one of the *trans* and *cis*-*β* complexes. As the yield of the primary reaction product is almost quantitative, it is concluded that the *meso*- and *rac*-*cis*-*β* isomers are not formed to a significant degree in the reaction of FeCl$_2$, KSCN, and prP$_4$.

Vibrational and Electronic Properties of *trans*-[Fe(NCS)$_2$(*rac*-prP$_4$)]. Complexes **1** and **3** were further characterized by vibrational and UV/vis absorption spectroscopy. The UV/vis spectrum of the *trans* compound **1** shows bands typical for an iron(II) low-spin complex. The $^1A_1 \rightarrow {}^1T_1$ transition is observed at 533 nm, and $^1A_1 \rightarrow {}^1T_2$ is found at 431 nm (see Figure S2 in the Supporting Information). In addition to these bands a charge-transfer band is found at 350 nm. Moreover, **1** and **3** were studied by vibrational spectroscopy, making use of ^{15}NCS isotopomers. The IR spectrum of *trans*-[Fe(NCS)$_2$(*rac*-prP$_4$)] (**1**) shows three isotope-sensitive bands, assigned to the antisymmetric CN stretch ν_{as}(CN) at 2099 cm^{-1}, the antisymmetric CS stretch ν_{as}(CS) at 818 cm^{-1}, and the antisymmetric Fe−N−C bend δ_{as}(FeNC) at 433 cm^{-1} (see Figure S3 and Table S1 in the Supporting Information). Upon isotope substitution, the ν_{as}(CN) signal shifts by about 28 cm^{-1} to 2071 cm^{-1}, the ν_{as}(CS) signal by 9 cm^{-1} to 807 cm^{-1}, and ν_{as}(FeN) by 7 cm^{-1} to 426 cm^{-1}. In the FT-Raman spectra the analogous symmetric vibrations could be identified (see Figure S4 and Table S1 in the Supporting Information): i.e., at 2105 cm^{-1} the symmetric CN stretch ν_s(CN), shifting by about 30 cm^{-1} on isotope substitution, as well as the symmetric CS stretch ν_s(CS) at 819 in the ^{14}N compound and 806 cm^{-1} in the ^{15}N complex. On the basis of these data a normal coordinate analysis was performed, which also is included in the Supporting Information.

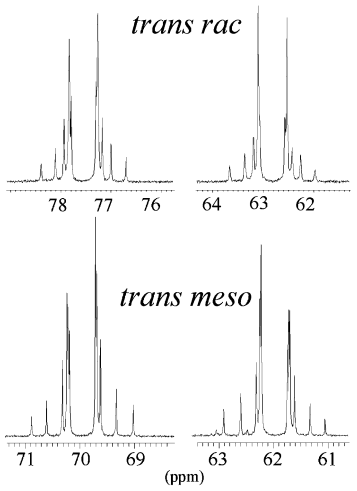

Figure 7. ^{31}P NMR spectra of *trans*-[Fe(NCS)$_2$(*rac*-prP$_4$)] (top) and *trans*-[Fe(NCS)$_2$(*meso*-prP$_4$)] (bottom).

Vibrational Properties of *cis*-α-[Fe(NCS)$_2$(*rac*-prP$_4$)]. In agreement with the loss of inversion symmetry, the vibrational selection rules valid for the *trans* complexes (symmetric ↔ Raman and antisymmetric ↔ IR) do not apply any more; i.e., both components of the Fe−NCS vibrations now can appear in the IR and in the Raman spectrum. The IR spectrum shows a small splitting of the ν(CN) stretches at 2112 and 2105 cm^{-1}, and the CS stretches correspond to a broad feature at 805 cm^{-1} (see Figure S5 in the Supporting Information). Other stretches could not be assigned, due to lack of isotope substitution data (Figure S5). In the Raman spectrum, the features at 2107 and 2103 cm^{-1} can be identified as in-phase and out-of phase CN stretches and the feature at 809 cm^{-1} as the split ν(CS) stretch (Table S1).

Summary

The tetraphos ligand prP$_4$ has been prepared and characterized by spectroscopy as well as X-ray structure

analysis of three isomeric iron thiocyanato complexes. In analogy to the synthesis of the linear tetraphos-I ligand, generating a mixture of *meso* and *rac*, prP_4 forms as a mixture of both diastereomers. The ratio between the two isomers varies from preparation to preparation; the factors influencing this composition could not be elucidated. Interestingly, two alternative routes of synthesizing prP_4 were found to occur stereoselectively.[2a,b] The identity of the resulting isomer of prP_4 and the origin of the observed stereoselectivities, however, are unclear in both cases.

Free prP_4 shows a ^{31}P NMR spectrum which is interpreted on the basis of an AA′XX′ spin system. To further characterize this ligand, three iron(II) bis(thiocyanate) complexes were crystallized and investigated by single-crystal X-ray structure determination and ^{31}P NMR spectroscopy. The compounds were found to be associated with two isomers, *trans*- and *cis*-α-[Fe(NCS)$_2$(*rac*-prP_4)]. The ^{31}P spectra of these complexes exhibit AA′XX′ patterns as well. Both isomers can also be distinguished on the basis of their vibrational spectra, showing typical differences in the region of the CN stretching vibrations. No evidence for formation of the *cis*-*β* isomer could be found, but the *trans*-*meso* compound could be identified by its ^{31}P NMR spectrum, showing a close similarity to that of the *trans*-*rac* complex. As demonstrated by NMR spectroscopy, octahedral *trans* coordination of [Fe(NCS)$_2$(*rac*-prP_4)] is preferred over the *cis* configuration, and the *cis* compound slowly converts into the *trans* isomer in solution. This is in agreement with DFT calculations, which predict that the *trans* isomer is 5 kcal lower in energy than its *cis* counterpart.

In summary, a complete analysis of the stereochemistry of the prP_4 ligand in mononuclear complexes has been obtained and the spectroscopic properties of the free ligand and its $Fe^{II}(NCS)_2$ complexes have been defined. Experiments are now underway to use this ligand in dinitrogen complexes of Mo(0) and W(0) relevant to nitrogen fixation.[6]

Experimental Section

a. Synthesis. All reactions were performed under an inert-gas atmosphere using Schlenk techniques. The solvents were dried and distilled under argon or dinitrogen gas. All other reagents were used without further purification. The sample preparation for vibrational, UV/vis, and NMR spectroscopy was carried out in a glovebox. ^{15}N-labeled thiocyanate (94.7%) was bought from VEB Berlin Chemie, Berlin Adlershof, Germany.

1-Chloro-2-(diphenylphosphino)ethane, $(C_6H_5)_2P(CH_2)_2Cl$. A 5.75 g portion (0.25 mol) of sodium was added to 250 mL of condensed ammonia at −78 °C. The solution turned immediately blue and was rapidly stirred for 1 h, until all sodium was dissolved. Then 32.75 g of triphenylphosphine (0.125 mol) was added over a 15 min period, and the resulting red solution was again stirred for 1 h. After the mixture was treated with 6.25 g (0.118 mol) of NH_4Cl (dried overnight at 100 °C) to destroy the C_6H_5Na formed as a cleavage product, it was stirred for another 1 h. The orange solution of sodium diphenylphosphide was added to a solution of 25 mL of $ClCH_2CH_2Cl$ in 25 mL of toluene at −78 °C. Then the solution was allowed to stand overnight to remove all NH_3 before 50 mL of toluene was added. The resulting mixture was washed twice with 40 mL of degassed water, the organic layer was dried over Na_2SO_4, and the solvents were removed with a rotary evaporator at 100 °C (water vacuum). Addition of 100 mL of hot absolute ethanol and subsequent slow cooling gave a white precipitate, which was recrystallized from ethanol. Yield: 41.6 g (67%). ^{31}P NMR (C_2D_5OD, 400 MHz): δ −17.85 ppm (s).

Dilithium 1,3-Bis(phenylphosphido)propane−Tetrakis(tetrahydrofuran), Ph(Li)PCH$_2$CH$_2$CH$_2$P(Li)Ph·4THF ("Lippp"). A 2.29 g portion of lithium metal (0.33 mol) was added to 60 mL of thf and the mixture cooled to 0 °C. Then a solution of 13.98 g of 1,3-bis(diphenylphosphino)propane (dppp; 0.0339 mol) in 80 mL of thf was added dropwise with stirring. The solution became orange-yellow and was refluxed by the use of an ultrasonic bath for 45 min, resulting in a dark red mixture. The warm mixture was separated from the precipitate by an injection needle to remove unreacted lithium metal. Then the volume of the filtrate was reduced to 20 mL and cooled to −78 °C. The resulting bright yellow powder was filtered and washed twice with 5 mL of cold diethyl ether. Recrystallization from thf gave yellow crystals. Anal. Calcd: C, 66.4; H, 8.6. Found: C, 66.1; H, 8.5. Yield: 12.9 g (68%).

1,1,4,8,11,11-Hexaphenyl-1,4,8,11-tetraphosphaundecane, Ph$_2$PCH$_2$CH$_2$P(Ph)CH$_2$CH$_2$CH$_2$P(Ph)CH$_2$CH$_2$PPh$_2$. An 8.0 g portion of $Ph_2PCH_2CH_2Cl$ (0.032 mol) dissolved in 100 mL of thf was added dropwise over a period of 1 h to an ice-cooled solution of Ph(Li)PCH$_2$CH$_2$CH$_2$P(Li)Ph·4THF (8.8 g, 0.016 mol) in 100 mL of thf. The solution was refluxed for 1 h and then cooled. A 30 mL portion of saturated NH_4Cl(aq) solution was added with vigorous stirring. The thf layer was decanted, and the aqueous layer was washed with 20 mL of thf. Both thf layers were combined and dried over $MgSO_4$, and the volume was reduced to 30 mL. After addition of 90 mL of ethanol the solution was allowed to stand overnight at −40 °C. Next day the white precipitate which formed was filtered and dried under vacuum. Anal. Calcd: C, 75.4; H, 6.5. Found: C, 75.4; H, 6.5. Yield: 7.4 g (68%). Mp: 106−108 °C.

***trans*- and *cis*-α Bis(isothiocyanato)(*rac*-1,1,4,8,11,11-hexaphenyl-1,4,8,11-tetraphosphaundecane)iron(II), [Fe(NCS)$_2$(*rac*-prP_4)].** A 48.6 mg portion (0.50 mmol) of potassium thiocyanate dissolved in 10 mL of ethanol was added dropwise to 31.7 mg (0.25 mmol) of $FeCl_2$ and 171.2 mg (0.25 mmol) of *rac*-prP_4, suspended in a mixture of 15 mL of ethanol and 10 mL of dichloromethane. The color changed to red, and the resulting precipitate was filtered. After some days red crystals were obtained from the filtrate. These were filtered and recrystallized from dichloromethane/ethanol. The *cis* isomer **3** could be crystallized as light red needles in low yields from solutions of the crude product, while the *trans* isomers **1** and **2** were obtained in better yields as dark red crystals from concentrated solutions of the crude product. The precipitate formed by the reaction yields a changing ratio for *trans* to *cis* isomer, on the basis of ^{31}P NMR of a solution of the primary reaction product. Elemental analysis of the crude product is as follows. Anal. Calcd: C, 63.1; H, 5.2; N, 3.3; S, 7.5. Found: C, 62.9; H, 5.2; N, 3.4; S, 7.5. The reaction is nearly quantitative.

b. Spectroscopy and Single-Crystal X-ray Structure Determinations. NMR Spectroscopy. NMR spectra were recorded on a Bruker Avance 400 pulse Fourier transform spectrometer operating at a ^1H frequency of 400.13 MHz using a 5 mm inverse triple-resonance probe head. References as external standards: H_3PO_4 85% pure, $\delta(^{31}P)$ 0 ppm; LiCl-saturated D_2O, $\delta(^7Li)$ 0 ppm; CH_3NO_2 neat, $\delta(^{15}N)$ 0 ppm. Samples were measured at 300 K. Spectral simulations were performed using the WinDNMR Calculation V7.1.6 software package by Hans J. Reich on a personal computer.

X-ray Structure Analysis. Intensity data were collected using a STOE imaging plate diffraction system with Mo Kα radiation. The structures were solved by direct methods using

(6) Habeck, C.; Hoberg, C.; Tuczek, F. To be submitted for publication.

SHELXS-97,[7] and refinement was performed against F^2 using SHELXL-97.[7] All non-H atoms were refined anisotropically. The hydrogen atoms were located with idealized geometry and refined with isotropic displacement parameters using a riding model. The crystals of compound **1** contain additional dichloromethane molecules as solvent which are extremely disordered. Because no reliable split model was found, the data were corrected for disordered solvent molecules using the squeeze option in Platon. The content of CH_2Cl_2 was estimated to about 0.5 per each formula unit.

UV−Vis Spectroscopy. The UV/vis spectra were recorded on a Analytik Jena Specord S100 spectrometer using a quartz cuvette under an inert gas atmosphere. The resolution was set to 1 nm.

IR Spectroscopy. Mid-IR spectra were obtained from RbI pellets using a Mattson Genesis Typ I spectrometer. Far-IR spectra were obtained from RbI pellets using a Bruker IFS 66 FTIR spectrometer. Both instruments were equipped with a Cryogenics helium cryostat, and all spectra were recorded at 10 K with resolution was set to 2 cm^{-1}.

Raman Spectroscopy. Raman spectra were obtained on a Bruker IFS 66/CS near-IR FT-Raman spectrometer at 270 K. The setup involves a 350 mW Nd:YAG laser with an excitation wavelength of 1064 nm. The samples were pressed into the groove of a holder which could be sealed with a glass plate to ensure inert gas conditions.

Acknowledgment. We want to thank the DFG SPP1118 (Tu58-13) for funding of this research.

Supporting Information Available: IR and FT Raman spectra of the compounds **1** and **3** as well as a UV−vis spectrum of **1**, procedures, the resulting force constants, and tables of calculated and experimental frequencies for a normal coordinate analysis of **1**, structure determination details, atomic coordinates, isotropic and anisotropic displacement parameters, and bond lengths and angles for all structures, and additional ^{31}P NMR spectra of the *cis*/*trans* conversion. This material is available free of charge via the Internet at http://pubs.acs.org.

OM030579K

(7) Sheldrick, G. M. SHELXS-97 and SHELXL-97: Program for the Solution and Refinement of Crystal Structures; University of Göttingen, Göttingen, Germany, 1997.